

Three-wave interaction among plasmons in a weakly coupled quasi-two-dimensional Fermi gas: Down-conversion of high-power terahertz radiation

J. P. Mondt,* Hyun-Tak Kim,[†] and Kwang-Yong Kang[‡]

Telecommunications Basic Research Laboratory, ETRI, Taejeon 305-350, Korea

(Received 4 August 1999; revised manuscript received 8 May 2000)

It is shown that, unlike in three dimensions, and as a result of their acoustic character, three plasmons of the same type in the same subband of a quasi-two-dimensional electron gas (Q2DEG) can satisfy the frequency matching conditions among themselves across different regimes of collisionality. The lowest frequency involved in the three-wave interaction can be tuned, through the use of segments of different impurity doping levels within the two-dimensional layer and through the total carrier density (gate voltage). A wide range of frequencies within the terahertz regime can thus be covered. The present theory is built on the flow equations based upon the Bhatnagar-Gross-Krook approximation as an extension of the Euler equations for quasi-two-dimensional electron layers for the low-frequency, collisional regime and the Lindhard theory based on the random phase approximation for the high-frequency, collisionless regime within the context of kinetic theory for an arbitrary Fermi-Dirac distribution. The mode-coupling equations show the possibility of generating plasmons in the terahertz range through frequency difference generation, yielding nonlinear growth within about 1 to 2 ps. The criterion for parametric instability based on one pump plasmon is also given. It is shown that the quasi-two-dimensional pump plasmon needed for the three-wave interaction within the Q2DEG found in this paper can be resonant with a three-dimensional plasmon in the bulk with a wave number corresponding to the peak of stimulated Raman scattering against plasmons for some parameters corresponding to a low-gap semiconductor. The dependence of the terahertz amplitude and rise time on the three-dimensional stimulated Raman scattering process providing the pump plasmon in the quasi-two-dimensional layer is quantified.

I. INTRODUCTION

Efforts to create a tunable, high-power, cw source of terahertz radiation through the excitation and subsequent grating-induced radiative decay of plasmons in quasi-two-dimensional electron gases (Q2DEG's) have widely been recognized for their potential.¹⁻⁶ The most extensively developed and interesting scenarios are based on the excitation of current-driven^{1,2} instabilities in a single layer or pair of counterstreaming layers, on the field-induced instability in a superlattice of alternating electron and hole layers,³ or on the shallow-water wave type electron plasma instability in the short field effect transistor.⁴⁻⁶ For the current-driven or field-induced methods it is not clear whether the fields required for acceleration of the carriers inevitably cause a degradation of the plasma or whether nonradiative decay of plasmons through acoustic phonons is too strong a competitive process. The strongly coupled nature of the $\text{Al}_x\text{Ga}_{1-x}\text{As}/\text{In}_x\text{Ga}_{1-x}\text{As}$ system considered for the short field effect transistor as well as for $\text{GaAs}/\text{Ga}_x\text{Al}_{1-x}\text{As}$ systems aimed for in the work on two-stream instability strictly speaking invalidates the application of the random phase approximation, thus also of a fluid-dynamical description. The strongly coupled nature of the plasma may well be a limiting factor in efforts for the practical realization of these methods by limiting the lifetime of plasmonlike structures to microdynamical time scales associated with the unscreened many-body system. This theoretical point^{7,8} is underscored experimentally⁹ in the case of optically excited plasmons in $\text{Al}_x\text{Ga}_{1-x}\text{As}/\text{GaAs}$ heterojunctions. Their quick decay was attributed to strong carrier-carrier interactions. Hence, both

theoretical and experimental arguments seem to favor the use of *weakly coupled* Q2DEG's for the generation of plasmons, to which case we restrict ourselves in this work [$r_s^2 \ll 1$, $r_s \equiv k_s/(2k_F)$, where k_F and k_s are the Fermi and screening wave numbers, respectively].

Particularly, we consider the *coherent* excitation¹⁰⁻¹² of plasmons as this method has several advantages. First, the level of excitation can be adjusted more readily by controlling the driver. Second, parametric excitation does not rely on the drift velocity as the sole source of free energy. Third, by varying the parameters (carrier density, pump frequency, temperature, drift velocity, doping concentration) the terahertz frequency could be tuned. To avoid the need for bulk acceleration that is necessary for two-stream instability but keep the advantage of high power through exploiting the long-range, collective interactions in the plasma, long-pulse, high-power, tunable THz radiation may be achieved by the application of *stimulated Raman scattering* (SRS) to nonmetallic media. Carrier densities of even intrinsic semiconductors such as InSb are experimentally known¹³ to be increased within 1 ps to about 10^{18} cm^{-3} through the application of a CO_2 laser ($\lambda \approx 10.6 \text{ } \mu\text{m}$) in the 100–200 MW/cm^2 power range and at a laser frequency below the intrinsic gap but above the expected range of subintrinsic peaks in the optical conductivity usually attributed to phonon activity. Laser power levels of several tens of MW/cm^2 are sustainable over much longer periods without damage to the crystal. Stimulated Raman scattering in InSb has also been established,¹⁴ while stimulated Raman scattering against the LO phonon and coupled LO-phonon-plasmon modes in GaP has long been known to produce extremely high gain, exceeding gains

from a/o CS_2 , LiNbO_3 , and potassium dihydrogenphosphate (KDP).¹⁵ It has long been recognized¹⁶ that SRS at intensities $>10 \text{ MW cm}^{-2}$ can produce Stokes wave intensities approaching those of the incident laser beam. In the case of InSb stimulated Brillouin scattering is known to interfere with SRS after about 1 ns. Numerical simulations¹⁷ indicate that such interference may be due to the local violation of the condition, necessary for propagation of the plasma wave and idler, that the carrier density be less than one-quarter critical. Therefore, a material with a slightly higher intrinsic gap may overall be preferable despite a lower relative power efficiency because of a higher down-conversion ratio. It is not the purpose of the present paper to specify a particular experimental configuration by which SRS in three-dimensional media could be exploited to excite the pump plasmon in the Q2DEG required for the presently discussed three-wave interaction. However, a numerical example is worked out based on a material with an energy gap and other material properties similar to InAs because of its low gap (0.35 eV at room temperature, 0.4 eV at 100 K without doping, and a reduction by less than 0.1 eV for doping concentrations not exceeding 10^{18} cm^{-3}).¹⁸ This may enable, under certain circumstances, the use of a laser wavelength down to as low as $4.2 \mu\text{m}$, although the experimentally obtainable power seems to be an open question. The plasmon frequency from three-dimensional SRS would only be moderately tunable, as it depends on three-dimensional parameters and moreover has an optical character; it also tends to be slightly above the desired THz range of (linear) frequencies between 0.2 and 2.0 THz. Therefore, *moderate down-conversion and a method for tuning* would be desirable. We stress, however, that on the one hand, to the best of the authors' knowledge the usefulness of InAs for this purpose is not established, while on the other hand, the physics of the currently found three-wave interaction among plasmons in Q2DEG's does not depend on the use of stimulated Raman scattering against plasmons, nor is it the focus of the present communication.

It is the main purpose of this paper to show that conditions for three-plasmon interaction within the electron (hole) plasma pertaining to one subband in a Q2DEG can be fulfilled, and that this offers the possibility to achieve down-conversion and tuning of high-power, three-dimensional longitudinal waves. Because of the limited range of the plasma frequency in three dimensions, and because of the weak and concave dependence on wave number of the three-dimensional plasma frequency, three-wave interaction among plasmons in a three-dimensional isotropic plasma is known to be impossible.¹² However, plasmons in Q2DEGs have an acoustic character, with a \sqrt{k} behavior of the frequency for small wave number. Furthermore, the dispersion curve has an inclination point at the screening wave number beyond which it is slightly convex, while the group velocity of the high-frequency plasmons with finite k/k_s is higher than what would be predicted from hydrodynamic theory. The latter property is caused by a difference in the electron (or hole) sound speed corrections in the collisional and collisionless regimes because of a difference in the rate of approach towards isotropy of the stress tensor relative to the oscillation frequency. If the rate of approach towards isotropy is higher than the oscillation frequency the pressure perturbation is isotropic within the Q2DEG, hence two-

dimensional, and (for low temperature, $T/T_F \ll 1$) the electron sound velocity is $s \approx v_F/\sqrt{2}$; if instead the rate of approach towards pressure isotropy is lower than the oscillation frequency the dynamics is essentially that of a one-dimensional, collisionless shock wave and the sound speed is closer to v_F . A third, and, as it turns out, more important factor contributing to three-wave interaction in the terahertz regime is the role of the linear momentum relaxation rate (ν_c) as a sink of momentum, but not of particle number density, thus providing an offset to the square of the real frequency ($\omega^2 \rightarrow \omega^2 - \nu_c^2/4$) in addition to a linear damping ($\gamma \approx -\nu_c/2$). That the conditions for three-wave interaction can be fulfilled is illustrated in Figs. 1 and 2. As a result of the offset the real phase velocity of the low-frequency plasmon varies over a range that can include the high-frequency plasmon group velocity within the terahertz regime for moderate values of the mobility, i.e., typically several thousands of $\text{cm}^2/(\text{Vs})$, while at the same time the frequency is tunable through the electron mobility (hence through the neutral impurity doping level) and through the total carrier density (i.e., gate voltage).

In addition to the generic process of three-plasmon interaction we also discuss a specific mechanism for producing high-frequency pump plasmons in the Q2DEG as an example of a possible application. When moving at close distance ($d \ll k^{-1}$) past a Q2DEG, a three-dimensional longitudinal wave interacts electrostatically with the Q2DEG charge carriers as if the wave occurs within it. This can be seen from the quasi-two-dimensional Poisson equation,¹⁹ of which the Green function after Fourier transformation in the coordinates tangential to the planes is given by

$$g(z, z_0) = (2k)^{-1} \exp(-k|z - z_0|), \quad (1)$$

where the exponential factor is non-negligible for any two points at vertical coordinates (z) differing by not substantially more than k^{-1} . Consequently, when its frequency and wave number match those of a plasmon in the Q2DEG it will be able to propagate as a quasi-two-dimensional plasmon there. As will be shown, a plasmon with frequency and wave number corresponding to the peak (backscatter) of SRS produced by a laser source with a (vacuum) wavelength of $4.2 \mu\text{m}$ in a three-dimensional medium with a refractive index $n_{r,3D} = 3.5$ can be resonant with a two-dimensional plasmon in an InSb layer for wave numbers of the order of the screening wave number, while at the same time conditions are manifestly fulfilled for three-wave interaction within the layer and while the grating is sufficiently close by to achieve radiative decay (cf. Figs. 3 and 4).

In passing it is noted here that the use of InSb as both the Q2DEG and the 3D medium is complicated for the case of SRS against plasmons because the peak wave number, being twice the wave number of the laser in the medium, is necessarily rather much lower than the screening wave number of Q2DEG's for moderate densities because of the extremely low-energy gap of InSb (0.17 eV at 300 K, 0.23 eV at 77 K), whereas the carrier density of the 3D medium is close to one-quarter critical. The collision frequency in the case of InSb as the 3D medium is just above the terahertz frequency (see Fig. 5), casting further doubt on the feasibility to use InSb. Therefore, although electron-neutral collisions, as-

sumed here to limit the mobility, typically make the distribution function isotropic after just one collision, important kinetic corrections must be expected in the case of InSb. As shown in Fig. 5, apart from the aforementioned difficulties it is possible to obtain three-plasmon resonance also in this case, while the intensities obtained for any given pump wave exceed those in the case of InAs precisely because of the closeness of terahertz and collision frequencies.

Returning to the InSb-InAs system described above, the terahertz radiation is shown to be tunable across a wide portion of the terahertz frequency range through variation of the carrier density and, more importantly, impurity concentration across segments of the layer, thereby allowing the use of the linear momentum relaxation rate for tuning. However, the terahertz power can only be quantified in terms of the power of the three-dimensional pump wave, the former depending quadratically on the latter. For the main purpose of the paper the specific nature of the three-dimensional longitudinal pump wave does not matter as long as it resonates. However, for the present purpose we restrict considerations to SRS against plasmons.

The organization of the paper is as follows. In Secs. II and III we derive the dispersion relations for plasmons in the collisionless, high-frequency regime as described by kinetic theory based on the random phase approximation and in the collisional, hydrodynamic regime as described by a Bhatnagar-Gross-Krook extension of the quasi-two-dimensional Euler equations, respectively. In Sec. IV we address the possibilities to obtain exact frequency matching. In Sec. V mode-coupling equations are derived based on a continuum description of the essential convective nonlinearities. In Sec. VI the nonlinear evolution is discussed, based on the nonlinear equations with full incorporation of linear damping, driving forces, and mode coupling for the case of frequency difference generation (FDG). The condition for parametric instability is also derived. In Sec. VII we present the numerical analysis on the creation and use of three-dimensional plasmons obtained from SRS as pump plasmons in the Q2DEG within this dynamical context. We end with concluding remarks.

II. HIGH-FREQUENCY PLASMON DISPERSION EQUATION

Within the context of the random phase approximation for the case of a spin-independent electron distribution the dispersion relation for a fully collisionless plasmon can be derived from the Schrödinger equation for the density operator²⁰ with the Hamiltonian

$$\hat{H} = \frac{\hbar^2}{2m} \Delta - e\varphi(t, \vec{r}), \quad (2)$$

subject to linearization about a homogeneous dynamical equilibrium, $\rho = \rho_0 + \delta\rho$, where ρ_0 only depends on $\vec{R} \equiv \vec{r}_1 - \vec{r}_2$. The density operator ρ_0 is related to the equilibrium electron momentum distribution by

$$n_0(\vec{p}) = N_e \int \rho_0(\vec{R}) \exp(-i\vec{p} \cdot \vec{R}) d^2x, \quad (3)$$

where N_e is the total number of electrons. As the occupation number of quantum states of electrons with definite values of the momentum and spin component, the number of states in an element d^2p of momentum space and with either value of the spin component is $2d^3p/(2\pi\hbar)^2$; hence the electron distribution function is given by $f(\vec{p}) = 2n(\vec{p})/(2\pi\hbar)^2$. After Fourier decomposition $\tilde{\psi} = \psi \exp(-i\omega t + i\vec{k} \cdot \vec{x})$, where \vec{x} is the spatial coordinate in the plane and z is the distance to the plane, the density response to a fluctuation in the electrostatic potential $\tilde{\varphi}$ is obtained in the usual manner²⁰ as

$$\tilde{n} = \frac{e\tilde{\varphi}}{\hbar} \int d^2p \frac{f(\vec{p} + \hbar\vec{k}/2) - f(\vec{p} - \hbar\vec{k}/2)}{\omega - \vec{k} \cdot \vec{p}/m}, \quad (4)$$

with the Landau prescription for the pole. The Fermi-Dirac distribution function may be written²¹ as a convolution over its zero-temperature limit $f_0 = 2/h^2 \theta(\mu' - p^2/2m)$, where θ is the Heavyside function and

$$f = \frac{\beta}{4} \int_0^\infty d\mu' \frac{f_0(\mu' - p^2/2m)}{\cosh^2\left[\frac{1}{2}\beta(\mu - \mu')\right]}, \quad (5)$$

where $\beta \equiv 1/(k_B T)$. The density response and electrostatic potential fluctuation are also related through the quasi-two-dimensional Poisson equation¹⁹ for free oscillations in a plane under the influence of the (three-dimensional) electrostatic potential, i.e.,

$$(\partial^2/\partial z^2 - k^2)\epsilon\varphi(\vec{k}, z, \omega) = -2\pi e k^{-1} \tilde{n}(\vec{k}, \omega) \exp(-k|z|), \quad (6)$$

where ϵ is the dielectric function. For the purpose of deriving the three-wave interaction among Q2DEG plasmons we may set $z=0$. Substituting Poisson's equation into the dynamical response and performing the integration over momentum prior to the convolution, Eqs. (4) and (6) lead to the following dispersion relation:

$$0 = 1 + \frac{\pi e^2}{2\epsilon\hbar k} \beta \frac{2}{h^2} \int_0^\infty d\mu' \frac{(J^+ - J^-)}{\cosh^2\left[\frac{1}{2}\beta(\mu - \mu')\right]}, \quad (7)$$

where we defined

$$J^s \equiv \int d^2p \frac{\theta(\mu' - p^2/2m)}{\omega_s - \vec{k} \cdot \vec{p}/m}, \quad (8)$$

with $s = +, -$ and $\omega_\pm \equiv \omega \pm \hbar k^2/(2m)$. The integration over the angle of the momentum can be performed to yield

$$J^s = \frac{m}{k} [A_+^{(s)} - A_-^{(s)}], \quad (9)$$

where

$$A_\pm^{(s)} \equiv \int_{|p_x| \leq p_M} dp_x \left[\ln\left(\frac{m\omega_s}{kp_M(p_x)}\right) \pm 1 \right]. \quad (10)$$

Here, $p_M \equiv (p_\mu^2 - p_x^2)^{1/2}$ with $p_\mu \equiv (2m\mu')^{1/2}$. Use of the substitution $x(\theta) = \sin(\theta)$ on $\theta \in (-\pi/2, \pi/2)$ followed by the inverse of $x(\theta) = \tan(\theta/2)$ that is monotonic on $(0, \pi/2)$ yields

$$A_+^{(s)} - A_-^{(s)} = 2\pi p_\mu [\tilde{v}_{\phi,s} - 2\pi(\tilde{v}_{\phi,s}^2 - 1)^{1/2}], \quad (11)$$

where the tilde in $\tilde{v}_\phi \equiv \omega/(kv_\mu)$ denotes normalization of the phase velocity in units of v_μ and $\omega_\pm \equiv \omega \pm \omega_q$, with $\omega_q \equiv \hbar k^2/(2m)$. The resulting dispersion equation is

$$0 = 1 + \frac{k_{TF}}{k} \left\{ (1 + e^{-\beta\mu})^{-1} + \frac{\beta}{8\omega_q} \int_0^\infty \frac{d\mu'}{\cosh^2[\beta(\mu - \mu')/2]} \right. \\ \left. \times [(\omega_-^2 - k^2 v_{\mu'}^2)^{1/2} - (\omega_+^2 - k^2 v_{\mu'}^2)^{1/2}] \right\}, \quad (12)$$

where $v_{\mu'}$ is the Fermi velocity corresponding to the chemical potential μ' . $k_{TF} \equiv 2me^2/(\hbar\bar{\epsilon})$ is the Thomas-Fermi wave number corresponding to the average dielectric constant $\bar{\epsilon}$ of the semiconductor and insulator. Without the dependence on μ' of the numerator of the integrand the integration would just yield the overall multiplier $(1 + e^{-\beta\mu})^{-1}$ for the entire term $\propto k_{TF}/k$. Thus finite temperature would only have an exponentially small effect in the degenerate regime; with it, however, electron plasmons in the sound wave regime ($k \gg k_{TF}$) are affected by wave-particle resonance, in particular, Landau damping.

It has been shown²² that screening and hence the effective k_{TF} are modified by nearby conductors on both sides of the Q2DEG. In the presence of a nearby grating, needed for radiative plasmon decay, the insulator thickness is limited by the distance d_{ins} of the Q2DEG to the grating. On the other hand, the thickness d_{sc} of the semiconductor would be limited by enhanced levels of the charge carrier density in it, as in the case of SRS against plasmons. The full expression for the modification is $k_{TF} \rightarrow k_{TF} 2\bar{\epsilon}/[\epsilon_{ins} \coth(kd_{ins}) + \epsilon_{sc} \coth(kd_{sc})]$.

Equation (12) will be used in the numerical work. Its form illustrates that finite temperature manifests itself mainly through distributing the relevant Fermi velocity over a range of the order of the thermal velocity. It is clear that finite temperature effects are most important when the (Doppler-shifted) phase velocities approach the Fermi velocity v_μ , which occurs for $k \gg k_{TF}$. As will be shown in the Appendix, the integral equation can be approximated by a local equation provided $T \ll T_F$ and the thermal velocity is small compared with the difference between v_μ and $v_{\phi,s}$ for $s = +, -$. The latter condition is the most restrictive; when not met Landau damping sets in. The local equation in its simplest form tends to agree quantitatively even for rather high $T/T_F < 1$ up to $k \approx k_{TF}$, but for realistic values of r_s it suddenly breaks down for wave numbers comparable to the Thomas-Fermi wave number (see Fig. 6). The authors do not know whether Eq. (12) for arbitrary temperature or its mathematical equivalent exists in the literature to date. It is used here because, in addition to demonstrating the importance of Landau damping for $k > k_{TF}$ and in addition to our interest in finite T/T_F for room-temperature applications, the pump waves in the three-plasmon interaction must have finite

k/k_{TF} , while small errors in the difference of pump and idler frequencies magnify in the expression for the resonance frequency. As discussed in the Appendix, its lowest-order approximation reduces to the more familiar forms²³ through the Taylor expansion for small k/k_{TF} .

III. LOW-FREQUENCY PLASMON DISPERSION RELATION

The description of the low-frequency plasmon in principle involves the nonlinear integro-differential kinetic equations with full incorporation of electron-electron and unlike-species collision terms. For simplicity we will adhere to the Euler equations for a quasi-two-dimensional Fermi gas¹⁹ of spin 1/2 augmented by a velocity drag term based on the Bhatnagar-Gross-Krook (BGK) model^{24,25} for the linear momentum relaxation processes. The coupling of fluctuations in the impurity and phonon distributions back onto the electrons is ignored. Linear momentum relaxation through collisions between different species also has an effect of creating pressure isotropy in their time scale through the randomization of the specific velocities. However, because electron-electron collisions conserve total electron momentum, their effect on momentum is mostly indirect, although it has been reported that they sometimes do contribute to mobility, specifically in narrow wires, where they cause an increase in electron collisions with the wall. Two collisional rates have to be distinguished, at least in principle, i.e., the linear momentum relaxation and the pressure anisotropy relaxation rate. The latter rate is the sum of the former and the $e-e$ collision rate, although practically the $e-e$ collision rate does not play an important role (see next section). In the present BGK model of the low-frequency plasmon we consider the electron plasma as a Q2DEG coupled to the outside through the (three-dimensional) electrostatic field and through unlike-particle collisions.

The complete fluid-dynamical equations based on the BGK approximation are²⁴

$$D_t n + n \nabla \cdot \vec{u} = 0, \quad (13)$$

$$\left\{ D_t \vec{u}_s + \frac{\nabla \cdot \mathbf{P}}{mn} - \frac{e}{m} \vec{E} \right\}_k = \nu_{jk} (\vec{u}_j - \vec{u}_k), \quad (14)$$

where \vec{u} is the electron fluid velocity (species k), \mathbf{P} is the pressure tensor, on the right-hand side summation over all species $j \neq k$ is assumed, and $D_t \equiv \partial_t + \vec{v} \cdot \nabla$. The pressure gradient term in the case of a two-dimensional Fermi gas is equal to $(s_0^2/n_0) \nabla n$, where s_0 is the adiabatic sound velocity. ν_{jk} is the resistance coefficient²⁴ per mass density of species k against the drag exerted by species j and as such only depends on the collision frequency of species k with species j , the effective masses of species j and k , and the density of target species j . The linear momentum collision terms for the case of massive scattering targets lead to perturbations in the momentum balance that can be approximated by $-\nu \delta \vec{u}$, as only the electron species is perturbed. There is no counterpart in the continuity equation to the drag in momentum balance, because we only consider particle-conserving collisions. Because the low-frequency plasmon is described in the regime where the pressure perturbation is fully isotropic, no

viscosity term is included in the force balance. Density and electrostatic fields are also coupled through Poisson's equation [Eq. (6)]. Linearization and Fourier decomposition of the continuity equation and force balance yield in the absence of background mass (fluid) flow

$$-i\omega\tilde{n} + in_0k_j\tilde{v}_j = 0 \quad (15)$$

and

$$-i\omega\tilde{v}_i - \frac{iek_{\perp,i}\varphi}{m} + ik_i\frac{s_0^2}{n_0}\tilde{n} = -\nu_c\tilde{v}_i. \quad (16)$$

Substituting Poisson's law into the inner product of force balance with \vec{k} , and eliminating the fluid velocity through the continuity equation, we find the dispersion equation

$$\omega^2 + i\nu_c\omega = \frac{2\pi e^2 n_0 |\vec{k}|}{\epsilon_r m} + k^2 s_0^2. \quad (17)$$

In terms of the screening wave number $k_s \equiv k_{TF} v_\mu^2 / (2s_0^2)$ the eigenfrequency may be written

$$\omega = [(k_s k + k^2) s_0^2 - \nu_c^2 / 4]^{1/2} - \nu_c / 2. \quad (18)$$

The sound velocity s_0 is, at any temperature, given by²⁶

$$s_0 = \frac{2P}{mn}. \quad (19)$$

Starting from the grand-canonical thermodynamic potential for an ideal Fermi gas with spin 1/2 over a surface area A ,

$$\Phi_{FD} = -\frac{mA}{\pi\hbar^2} \beta^{-2} \int_{-\beta\mu}^{\infty} dx \ln(1 + e^{-x}), \quad (20)$$

the pressure, as $P = -\Phi_{FD}/A$ ($A \rightarrow 0$), is seen to have the following exact temperature dependence:

$$\frac{P}{P(T=0)} = 2(\beta\mu)^{-2} \int_{-\beta\mu}^{\infty} \ln(1 + e^{-x}) dx, \quad (21)$$

where $\beta \equiv 1/(k_B T)$. This determines the temperature dependence of the sound velocity through Eq. (19) and thereby also that of the screening wave number $k_s = k_{TF} v_\mu^2 / (2s_0^2)$.

The logarithm in the above integral can be analytically determined (convergence radii are 1) without approximations by expanding the logarithm in $\ln(1 + e^{-x}) = \ln(1 + e^x) - x$ for small e^x in the negative domain and expanding $\ln(1 + e^{-x})$ for small e^{-x} in the positive domain. This yields

$$s_0^2 = \frac{1}{2} v_F^2 \left\{ 1 + \left[\frac{1}{3} \pi^2 - 2 \sum_{n=1}^{\infty} (-1)^{n-1} z^{-n} \right] (\beta\mu)^{-2} \right\}, \quad (22)$$

where the sum involving the fugacity $z \equiv e^{\beta\mu}$ can be approximated by its first term even for the case when $T \approx T_F$.

IV. FREQUENCY MATCHING

While the electron-electron scattering rate with regard to the energy of a quasiparticle is quadratic in T/T_F ,^{27,28}

$$\nu_{e-e} = \frac{\pi}{8} \tau^2 \left[\ln(\tau) + \frac{\ln(8)}{2} - 0.083 \right], \quad (23)$$

where $\tau \equiv T/T_F$, and the electron-electron momentum anisotropy relaxation rate for degenerate systems is reported to be much slower than ν_{e-e} as given above, namely a factor $\propto \tau^2$ slower, except within a cone of order $\sqrt{\tau}$.²⁹ In the present work we will therefore neglect the electron-electron collisions altogether. The three-wave interaction, then, is limited to nonideal systems. Because the electron momentum relaxation rate due to all other types of collisions affects the momentum of the electron fluid as a whole, it is necessary to keep this rate as low as possible in order to prevent strong damping ($\propto \nu_c/2$). This prompts consideration of the regime $\omega < \nu_c < \omega_0$. The linear momentum relaxation reduces the real frequency for a given $k < k_{TF}$, thereby reducing the phase velocity of the low-frequency plasmon such that it becomes equal to the group velocity of the pump plasmon(s), which is roughly the phase matching condition. As can be seen from the position of the participating modes in the linear dispersion curves (cf. Fig. 2), the idler wave is rather close to the pump, such that a Taylor expansion of the difference of their frequencies is allowed for purposes of illustration. However, in the numerical calculations the exact expressions for the pump and idler frequencies are taken into account, as the danger otherwise might be that in relation to the (much) lower excited frequency the error in the Taylor expansion is not negligible. Let the group velocity of high-frequency plasmons near the pump and idler be $v_{g,h}$. Then, within the context of the Taylor expansion, wave number k and frequency ω of the low-frequency mode both match when $k v_{g,h} \approx \omega$, i.e.,

$$k^2 (v_{g,h}^2 - s_0^2) \approx k k_s s_0^2 - \nu_c^2 / 4. \quad (24)$$

Because $v_{g,h} > v_F$ as the pump wave has to be in the purely oscillatory regime while, except for highly nondegenerate regimes, $s_0 \approx v_F / \sqrt{2} < v_F$, there is a solution to the resonance condition provided the plasma frequency in the absence of linear momentum relaxation exceeds half the linear momentum relaxation rate. Note that the plasmon frequency in the presence of linear momentum relaxation is reduced, such that the required inequality for pressure isotropy on the time scale of the excited frequency can be met. From Eqs. (18) and (61) the wave number is found to be

$$k = \frac{k_s}{2[v_{g,h}^2/s_0^2 - 1]} \left(1 \pm \left\{ 1 + \left[1 - (v_{g,h}^2/s_0^2) \frac{\nu_c^2}{k_s^2 s_0^2} \right] \right\} \right)^{1/2}, \quad (25)$$

while the threshold linear momentum relaxation rate is

$$\nu_c \leq (v_{g,h}^2/s_0^2 - 1)^{-1/2} k_s s_0. \quad (26)$$

Inclusion of linear momentum relaxation in the high-frequency plasmon dispersion equation does not significantly modify the frequency matching condition, because in order of magnitude this modification could be estimated from the same effect on a mode of higher frequency given by the Euler equations with a BGK term added. From the above-

mentioned threshold condition with $v_{g,h}^2 \geq v_F^2 \approx 2s_0^2$, we obtain $v^2/4 \leq k_s^2 s_0^2/4 \leq 2k_s^2 s_0^2$. Therefore, up to an error of relative order $(v_v/\omega_0)^2/8$,

$$\omega \approx \omega_0 \left(1 - \frac{v_c^2}{8\omega_0^2} \right), \quad (27)$$

where ω_0 is the high-frequency eigenfrequency in the absence of collisions. Applying this rough estimate we see that the frequency matching condition $\omega_0 - \omega_1 = \omega$ only acquires an additional term through BGK effects on the pump and idler by $-v_c^2/(8\omega_1^2)$ on the left, which is small compared with the excited frequency ω , because, as a prerequisite for the matching $\omega_1 \geq v_c$. Figure 2 indicates the positions on the dispersion curves in a typical example of a three-wave resonance.

V. MODE-COUPLING EQUATIONS

To analyze the mode coupling we will assume, for simplicity, one-dimensional perturbations in a fully degenerate Fermi gas. The high-frequency modes are only needed in a narrow portion of wave numbers, between idler and pump waves, in which we can take the dependence on wave number of frequency to be linear, as evidenced from the high-frequency dispersion equation. To avoid a very complicated nonlinear kinetic treatment we will represent the high-frequency modes by a dispersion equation that is linear as far as the dependence of frequency on wave number between pump and idler waves is concerned (although with an offset) and adopt otherwise the same nonlinear fluid equations as for the low-frequency modes. Implicitly we thereby approximate its *form* (as opposed to the *location* of the points on the dispersion curve) by that of the low-frequency dispersion equation. Eliminating the electrostatic potential from the fully linear Poisson equation [Eq. (6)] the normal modes a_L and a_H for the low- and high-frequency waves are combinations of the dynamical variables $\bar{n}/n_0 \sim \exp(ikx - i\omega t)$ and \bar{v}_x , i.e., $a = \bar{n}/n_0 + \lambda \bar{v}_x$, where in both low- and high-frequency cases the coefficient λ is determined by requiring a to be an eigenmode in the linear case, which yields

$$a_{L,H} = \frac{\bar{n}}{n_0} + \frac{k}{\omega_{L,H}^*} \bar{v}_x, \quad (28)$$

in which the $\omega_{L,H}$ are the eigenfrequencies of the low- and high-frequency modes, respectively, the latter being given by the fully kinetic dispersion relation. From the continuity equation the relation between the normal modes and the electron density perturbation is obtained, i.e.,

$$a_{H,L} = \left(1 + \frac{\omega_{H,L}}{\omega_{H,L}^*} \right) \frac{\bar{n}_{H,L}}{n_0}. \quad (29)$$

Turning to the nonlinear fluid equations, the nonlinearity involving the sound velocity, which vanishes when $s_0^2 \approx v_F^2$, will be neglected, and the only nonlinearities that remain are $\partial_x(nv_x)$ in the continuity equation and $v_x \partial_x(v_x)$ in force balance. Expressing the real variables (e.g., \tilde{n}_L) in terms of

the dynamical variables [in this example $\frac{1}{2}(\tilde{n}^{(0)} + \tilde{n}^{(1)})$ and its complex conjugate) and collecting terms with the same Fourier component, the following set of mode-coupling equations is obtained:

$$(\partial_t + i\omega_L)a_L = c_L^{(0,1)} a_H^{(0)} a_H^{(1)*}, \quad (30)$$

$$(\partial_t + i\omega_H^{(0)})a_H^{(0)} = c_H^{(1,L)} a_H^{(1)} a_L, \quad (31)$$

$$(\partial_t + i\omega_H^{(1)})a_H^{(1)} = c_H^{(0,L)} a_H^{(0)} a_L^*, \quad (32)$$

where the mode-coupling coefficients are given by

$$c_L^{(0,1)} = -\frac{ik_L}{16} \left(v_H^{(0)} + v_H^{(1)} + \frac{v_H^{(0)} v_H^{(1)}}{v_L^*} \right), \quad (33)$$

$$c_H^{(1,L)} = -\frac{ik_H^{(0)}}{16} \frac{\omega_L^*}{\text{Re}(\omega_L)} \left(v_H^{(1)} + v_L + \frac{v_L v_H^{(1)}}{v_H^{(0)}} \right), \quad (34)$$

$$c_H^{(0,L)} = -\frac{ik_H^{(1)}}{16} \frac{\omega_L}{\text{Re}(\omega_L)} \left(v_H^{(0)} + v_L^* + \frac{v_L^* v_H^{(0)}}{v_H^{(1)}} \right), \quad (35)$$

where $v_{\phi,H}$ and $v_{\phi,L}$ are the average phase velocity of the pump and idler waves, and the (complex) phase velocity of the low-frequency wave, respectively.

To simplify notation define

$$a_0 \equiv a_H^{(0)}, \quad a_1 \equiv a_H^{(1)}, \quad a_2 \equiv a_L, \quad (36)$$

$$c_{0,1} \equiv c_L^{(0,1)}, \quad c_{1,2} \equiv c_H^{(1,L)*}, \quad c_{0,2} \equiv c_H^{(0,L)}, \quad (37)$$

$$\omega_0 \equiv \omega_H^{(0)}, \quad \omega_1 \equiv \omega_H^{(1)}, \quad \omega_2 \equiv \omega_L, \quad (38)$$

and define moduli and phases for all amplitudes and coupling coefficients, $a_j = u_j e^{-i \text{Re}(\omega_j)t + i\phi_j}$, $c_{ij} = v_{ij} e^{i\theta_{ij}}$, the mode-coupling equations can be shown to be equivalent to the real equations

$$\partial_t u_0 = v_{12} u_1 u_2 \cos(\Phi + \theta_{12}), \quad (39)$$

$$\partial_t u_1 = v_{02} u_0 u_2 \cos(\Phi + \theta_{02}), \quad (40)$$

$$\partial_t u_2 = -\frac{1}{2} v_c u_2 + v_{01} u_0 u_1 \cos(\Phi + \theta_{01}), \quad (41)$$

$$\begin{aligned} \partial_t \Phi = & - \left[v_{12} \frac{u_1 u_2}{u_0} \sin(\Phi + \theta_{12}) + v_{02} \frac{u_0 u_2}{u_1} \sin(\Phi + \theta_{02}) \right. \\ & \left. + v_{01} \frac{u_0 u_1}{u_2} \sin(\Phi + \theta_{01}) \right], \end{aligned} \quad (42)$$

where $\Phi \equiv \phi_0 - \phi_1 - \phi_2$. From Eqs. (33)–(35) it follows that

$$\theta_{0,1} = \theta_{0,2} = -\pi/2 + \theta_c, \quad \theta_{1,2} = \pi/2 + \theta_c, \quad (43)$$

where $\theta_c \equiv \arg[1 + v_H v_L / (2|v_L|^2)]$ represents the effect of dissipation on the phases of the coupling coefficients.

VI. NONLINEAR EVOLUTION

Although linear damping is slow compared with the oscillation frequency of the high-frequency plasmons and thus

does not affect their dispersion relations, it is comparable to the linear damping of the low-frequency plasmons and the nonlinear time scales of evolution. Therefore, in the description of the nonlinear evolution of the three-wave system it is necessary to include linear damping for all plasmons. Furthermore, a model of the SRS driving force is required. To be specific, let us assume that in the absence of the mode coupling the overall effect of the driving force and losses on any driven high-frequency plasmon u_H is to bring and maintain its amplitude to a certain level $u_{H,m}$ at a characteristic rate $\nu_{H,d}$ and proportional to its relative deviation $u_{H,m} - u_H$ from it. Defining $\hat{\Phi} \equiv \Phi + \theta_c - \pi/2$ the dynamical system may then be written as

$$\partial_t u_0 = -v_{12} u_1 u_2 \cos \hat{\Phi} + \nu_{0,d} (u_{0,m} - u_0) - \frac{1}{2} \nu_c u_0, \quad (44)$$

$$\partial_t u_1 = v_{02} u_0 u_2 \cos \hat{\Phi} + \nu_{1,d} (u_{1,m} - u_1) - \frac{1}{2} \nu_c u_1, \quad (45)$$

$$\partial_t u_2 = u_0 u_1 \cos \hat{\Phi} - \frac{1}{2} \nu_c u_1, \quad (46)$$

$$\partial_t \hat{\Phi} = \sin \hat{\Phi} \left(v_{12} \frac{u_1 u_2}{u_0} - v_{02} \frac{u_0 u_2}{u_1} - v_{01} \frac{u_0 u_1}{u_2} \right). \quad (47)$$

As the relevant collisions are between electrons and neutral species within the framework of a BGK model we assume all three plasmons share the same ν_c while for the case of FDG we will take the rates $\nu_{d,H} \equiv \nu_d$ and asymptotic levels $u_{H,m} \equiv u_H$ to be the same for both high-frequency plasmons. Because the estimate $\gamma_{Landau} \approx -\text{Im}(\epsilon)/\partial_\omega \text{Re}(\epsilon)$ shows that the Landau damping is less than 1/1000 of the collisional damping for the cases studied here we approximate their damping rate by the collision rate ν_c , which when dominated by electron-neutral collisions as assumed here can be taken to be the same for all three waves. We consider the case when both high-frequency modes are driven through the use of two lasers with different wave numbers $k_{0,1}$ (hence different pump wave numbers in the Q2DEG) and the use of two separate slabs with different carrier density within a distance $d \leq k_{0,1}$ from and parallel to the Q2DEG, such that the three-dimensional plasma frequencies $\omega_{p,3D} \equiv (4\pi n_{3D} e^2)/(m_* \epsilon_{3D})^{1/2}$ are equal to the frequencies $\omega_{0,1}$, respectively. Alternatively, one slab with a gradient in the carrier density could be considered. No distinction will be made between the growth time of the three-dimensional stimulated Raman signals for the high-frequency modes. After an initial rise time (γ_{SRS}^{-1}) due to the startup of SRS in the 3D medium to a level for the amplitudes of the normal modes (u_i) that would be equal to a certain level u_m in the absence of the mode coupling a stationary state sets in. If the initial phase $\hat{\Phi}$ is set to zero it remains so during the evolution; if not it relaxes to zero typically in a fraction of 1 ps [Fig. 7(a)]. The time needed for the low-frequency plasmon to reach its asymptotic value typically is of the order of a picosecond or two [Fig. 7(b)]. Figure 8 shows the numerical solution for the asymptotic values of the ratio of the (dynamical) density perturbation of the low-frequency mode di-

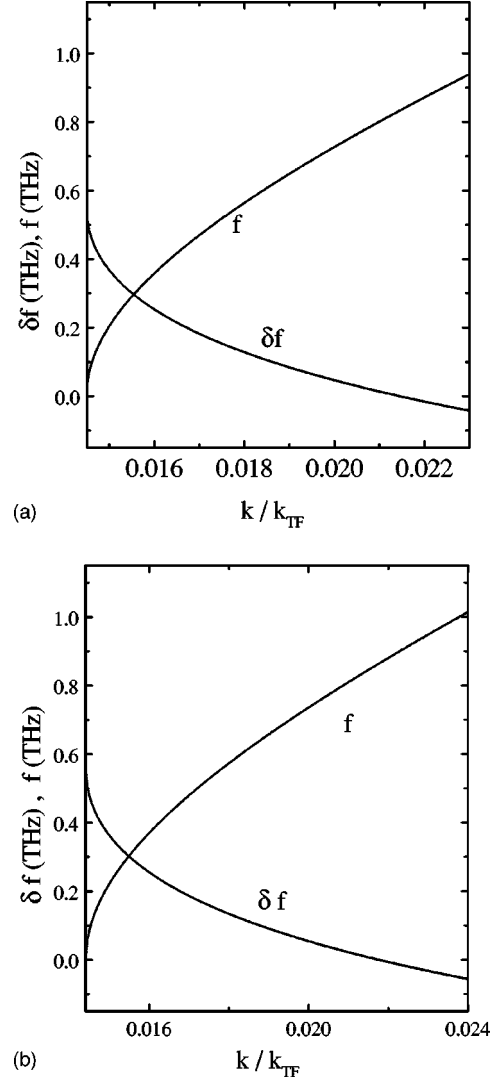


FIG. 1. Frequency mismatch and terahertz frequencies (both linear rather than angular) versus the ratio of the terahertz wave number divided by the Thomas-Fermi wave number for (a) $T=77$ K, and (b) $T=300$ K, for the case when the total carrier density $n_{total} = 2 \times 10^{12} \text{ cm}^{-2}$. The infrared dielectric constants of the insulator and semiconductor are chosen to be $\epsilon_{ins} = 3$ and $\epsilon_{sc} = 16$, respectively. The distances from the Q2DEG to the grating and to the illuminated portion of the semiconductor are $d_{ins} = 2000 \text{ \AA}$ and $d_{sc} = 1000 \text{ \AA}$, respectively. The pump wave number is chosen to correspond with the peak of SRS against plasmons ($k_0 = 2k_{laser} \approx 1.0472 \times 10^5 \text{ cm}^{-1} \approx 0.097k_{TF}$) for a 3D refractive index $n_{r,3D} = 3.5$ and a vacuum laser wavelength of $4.2 \mu\text{m}$. The wave number k_0 determines the pump frequency through the high-frequency dispersion relation. This frequency should equal the three-dimensional plasma frequency excited by SRS. Its (linear) value is $f_0 = 4.578 \text{ THz}$. The mobility was selected to be $\mu = 6708 \text{ cm}^2/(\text{V s})$. The semiclassical approximation for the mass dependence for narrow-gap semiconductors is adopted (Ref. 30), such that $m_* = 0.03$ for this total carrier density. The (linear) electron momentum relaxation frequency is therefore $f_c = 1.542 \text{ THz}$. The excited frequency is $f = 0.833 \text{ THz}$. The 0-subband density is taken (Ref. 30) to be $n = 0.67n_{total}$.

vided by that of the high-frequency mode in percentage as a function of both the strength and growth rate of the 3D SRS process as represented by the asymptotic normal mode amplitude of the high-frequency modes in the Q2DEG in the absence of mode

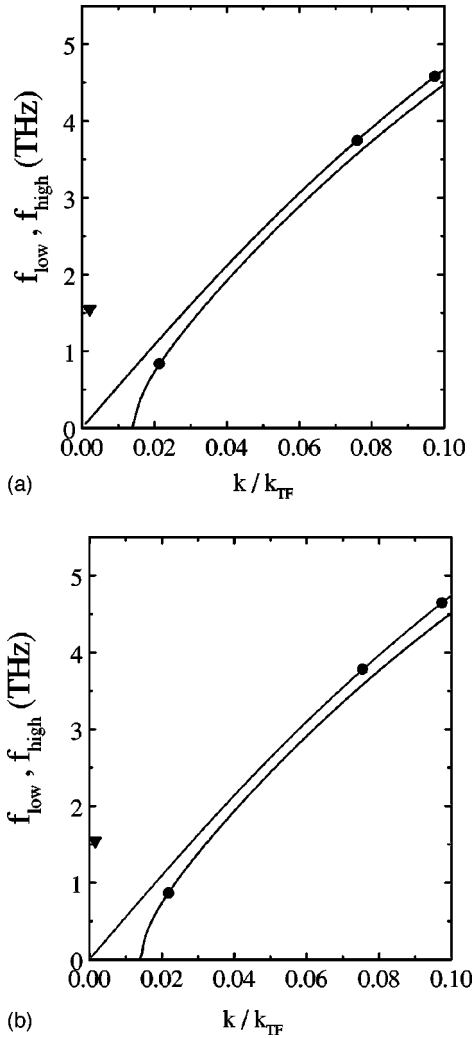


FIG. 2. Fast and slow wave dispersion relations showing the interacting triplet and the electron momentum relaxation frequency for (a) $T=77$ K and (b) $T=300$ K for the parameters pertaining to Fig. 1.

coupling. Additional losses due to the distance between the 3D medium and the Q2DEG and between the Q2DEG and the grating are not taken into account in Fig. 8 and amount to a multiplication of the ordinate by $e^{-k_H d_{sc}} e^{-k_L d_{ins}}$ (≈ 0.28 for the parameters of Fig. 8).

Finally, we give an analytical criterion for the onset of parametric instability (one driver only). Setting $\partial_t = 0$ in all dynamical equations we see that the asymptotic value of the normal mode of the pump wave $u_{0,\infty}$ corresponds to the condition for the marginal point of a purely growing instability for the envelope of the pump plasmon, i.e.,

$$u_{0,\infty} = \frac{v_c/2}{\sqrt{v_{01}v_{02}}}. \quad (48)$$

Then a steady state with nonzero $u_{2,\infty}$ transpires if and only if

$$u_{2,\infty} = \left(\frac{v_{01}}{v_{02}} \right)^{1/4} \left(\frac{[v_d(u_m - u_{0,\infty}) - v_c u_{0,\infty}/2]}{v_{02}} \right)^{1/2} \quad (49)$$

is real and nonzero, whence if and only if

$$\sqrt{v_{01}v_{02}u_m} > \frac{(v_d + v_c/2)(v_c/2)}{v_d}. \quad (50)$$

This criterion agrees with numerical solutions. However, the threshold is not met for the presently studied parameter set (see Fig. 3) chosen to obtain resonance with three-dimensional SRS in a moderately low-gap semiconductor.

VII. NUMERICAL ANALYSIS ON THE USE OF PUMP PLASMONS FROM STIMULATED RAMAN SCATTERING

In the numerical analysis we use a fit to the semiclassical approximation³⁰ for the dependence on total carrier density of both the effective mass and the density of the zeroth subband of a Q2DEG consisting of InSb. This approximation agrees closely with the more complete theory.^{31,32} For the electro-optical properties of the low-gap semiconductors InSb and InAs as three-dimensional media we refer to articles in a recent compendium.^{18,33}

Our main objective in this section is to demonstrate that SRS against plasmons in a three-dimensional medium adjacent to the Q2DEG may in principle be used for the generation of the high-frequency pump plasmons needed for the currently proposed three-plasmon interaction in a Q2DEG. This issue depends admittedly on the maximum obtainable power through SRS in three-dimensional media, which is ultimately an experimental issue beyond the scope of the present article. However, we show here that the resonance conditions, first between the three-dimensional plasmon and a Q2DEG plasmon with finite k/k_{TF} , and subsequently between the Q2DEG plasmon thus created and two lower-frequency plasmons, can be met, such that the lowest frequency plasmon is in the terahertz range and such that, through variation of total carrier density and impurity level, this frequency can be tuned across the terahertz range. Furthermore, the resonance between the three-dimensional plasmon and the Q2DEG plasmon of finite k/k_{TF} can be accomplished at peak SRS power (backscatter). Leaving aside considerations of manufacturability, we also show that these statements can be made not only for fairly low temperature (77 K), but also for room temperature ($T=300$ K).

The illumination by a laser of a frequency below the material's energy gap but at least a factor well over 2 above the plasma frequency associated with the charge carriers in the three-dimensional medium, and at a Poynting flux (S) below the breakdown voltage but exceeding the stability threshold for SRS would yield a spectrum of plasma waves peaking at the backscatter wave number $k_{p,3D} = 2k_{laser}$. In terms of the electric field amplitude of the laser light

$$E_0 = \left(\frac{8\pi S}{c\sqrt{\epsilon}} \right)^{1/2} \quad (51)$$

and assuming the predominance of collisional damping ($\nu_{c,3D}$) the threshold condition for the onset of SRS is given in the underdense regime by³⁴

$$\frac{eE_0}{\kappa m_* c} \left(\frac{n}{n_{cr}} \right)^{1/4} > \nu \frac{\omega_{p3D}}{\omega_1}. \quad (52)$$

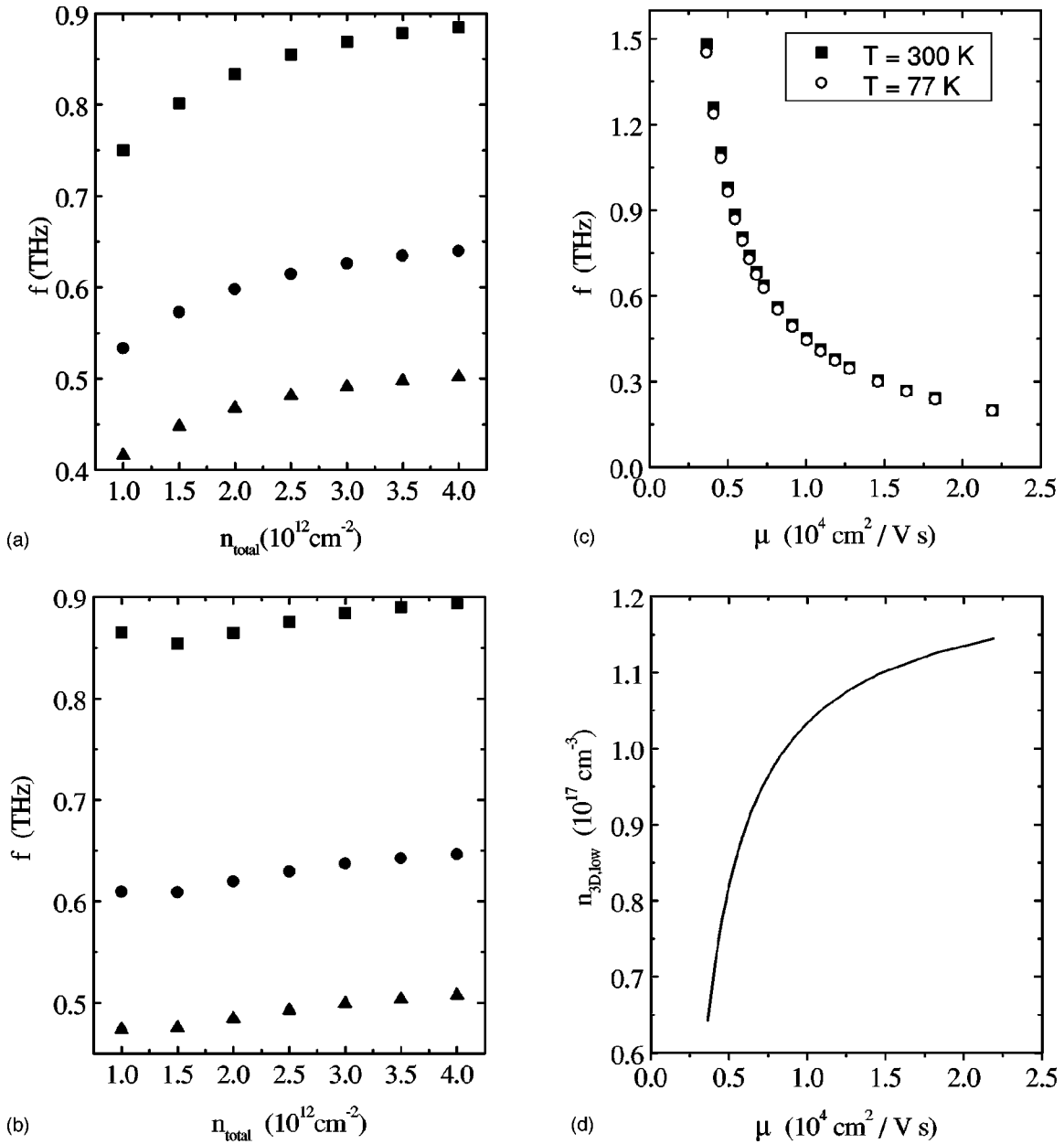


FIG. 3. Dependence of the terahertz frequency on the (total) carrier density for three different impurity contents including the choice for Figs. 1 and 2: (a) $T = 77 \text{ K}$, (b) $T = 300 \text{ K}$. Because the mobilities are assumed to be dominated by impurities they depend on carrier density through the Fermi velocity and the mean free path. Therefore we assume $\mu \propto 1/\sqrt{n}$. At a reference total carrier density of 10^{11} cm^{-2} the values of the mobility were taken to be 30 000 (solid squares), 40 000 (solid circles), and 50 000 (upward triangles) $\text{cm}^2/(\text{Vs})$. All other parameters are the same as in Figs. 1 and 2. Also, (c) its dependence on the mobility for $n_{\text{total}} = 3 \times 10^{12} \text{ cm}^{-2}$ for $T = 77 \text{ K}$ and $T = 300 \text{ K}$, and the same parameter setting. Finally, (d) the dependence on mobility of the required three-dimensional carrier density for the same parameter setting.

Provided a strip of the three-dimensional medium adjacent to the quasi-two-dimensional layer is excited such that the distance of the strip to the layer does not exceed the wave number of the excited three-dimensional plasmon, the two- and three-dimensional media can be considered as interpenetrating, as discussed before. A two-dimensional plasmon (ω_0, k_0) is then excited by the three-dimensional plasmon when $\omega_0 = \omega_{p,3\text{D}}$ and $k_0 = 2k_{\text{laser}}$. Because the group velocity of the two-dimensional pump (and idler) plasmon is low the phase velocity of the excited low-frequency plasmon should be considerably lower than the sound velocity of the low-frequency plasmon. Therefore, any excited low-

frequency plasmon must have a significant correction in the real frequency caused by the linear momentum relaxation rate. This can only happen if the relaxation rate is not too far removed from the lowest plasmon frequency. The sharpness of the resonance and the location of the triplet on the high- and low-frequency plasmon dispersion curves are illustrated in Figs. 1 and 2, respectively. As shown in Fig. 3 the terahertz frequency is tunable throughout a wide range by varying the total carrier density and (more important) the impurity level, such that the momentum relaxation rate itself is varied through the dependence of the mean free path on the total carrier density. Tunability could thus be achieved in

principle by varying the doping level in the Q2DEG from one segment to another, using the total carrier density (gate voltage) for fine tuning. That the frequency of the excited plasmon could be in the terahertz regime and that the relaxation rate satisfies the conditions $\omega/\omega_c \ll 1 \ll \omega_1/\omega_c$, albeit for the former inequality only marginally, is illustrated in Figs. 3 and 5. The parameters $\tau \equiv T/T_F$ and k_s/k_F are small as required (Fig. 4). Furthermore, these conditions are met while the illuminated area is within about one inverse pump wave number from the Q2DEG *and* while the grating is well within one inverse terahertz plasmon wave number from the Q2DEG [see Figs. 4(a), 4(b), and 5(b)]. The pump wave number in the Q2DEG is limited by the energy gap of the three-dimensional medium, for which in the present numerical results, we assumed a value not less than that of InAs, which is given by¹⁸

$$E_g = 0.415 - 2.76 \times 10^{-4} \frac{T^2}{T+83} \text{ eV}, \quad (53)$$

where T is in K ($0 < T < 300$). We assume here that the energy gap narrowing due to high doping levels is such that a value for the laser pump wavelength equal to $4.2 \mu\text{m}$ ($\approx 0.28 \text{ eV}$) is still allowable. Finally, we note that the results for pure InSb are limited to 77 K because of the laser wavelength of $8 \mu\text{m}$ and the low-energy gap of InSb.

VIII. CONCLUDING REMARKS

Three-wave interaction between three plasmons in the same subband of a weakly coupled, quasi-two-dimensional, Fermi gas of spin 1/2 was shown to be possible in principle across regimes of different collisionality. In three-dimensional plasmas three-wave interaction among electron plasmons is known to be impossible. The nonlinear evolution has been quantified through the derivation of the mode-coupling equations using a fluid approach to the convective nonlinearities. It was shown that SRS against plasmons at peak power (backscatter) through the use of a nearby three-dimensional semiconducting medium of a moderately narrow gap and a gradient in the charge carriers, or, alternatively, two parallel segments of different carrier concentration, could in principle provide plasmons with the correct wave numbers to generate a Q2DEG plasmon in the terahertz range.

One open question is the output power that is maximally obtainable in the three-dimensional SRS process, as this output power is input into the presently proposed three-wave interaction within the Q2DEG. The terahertz output power depends quadratically on it. In this work only the relation between input and output power within the quasi-two-dimensional plasma has been quantified. Therefore, the obtainable power levels are an open question depending on the experimentally achievable three-dimensional density fluctuation level of coherent longitudinal excitations. Given such a level the present theory predicts terahertz output through frequency difference generation. For the purpose of generating a suitable pump plasmon in the Q2DEG it is not essential that the SRS in the nearby three-dimensional medium be against plasmons, the only requirement being that the excited longitudinal mode must correspond to a solution of the quasi-two-dimensional dispersion equation for high-

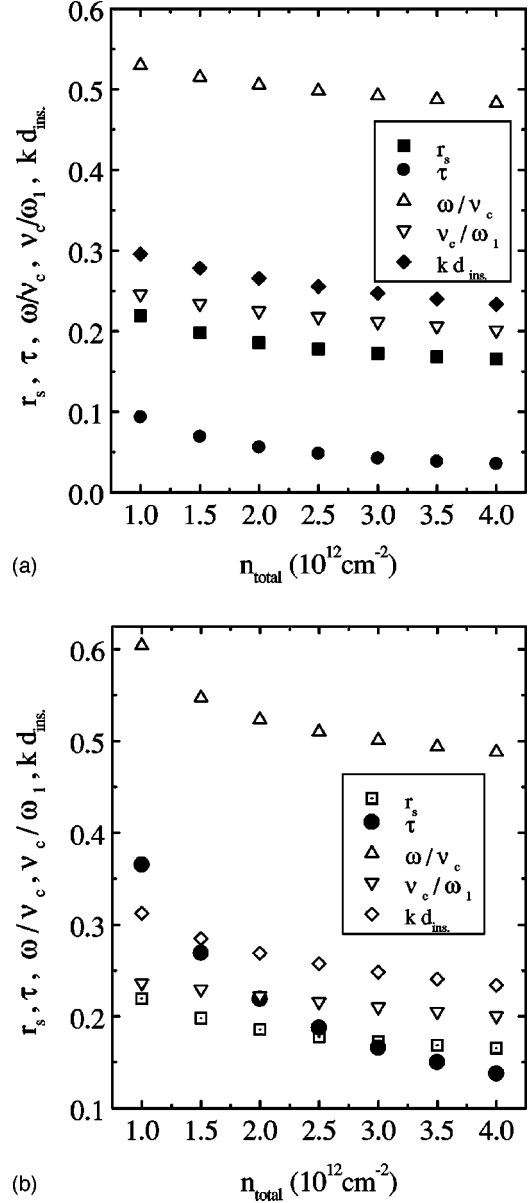
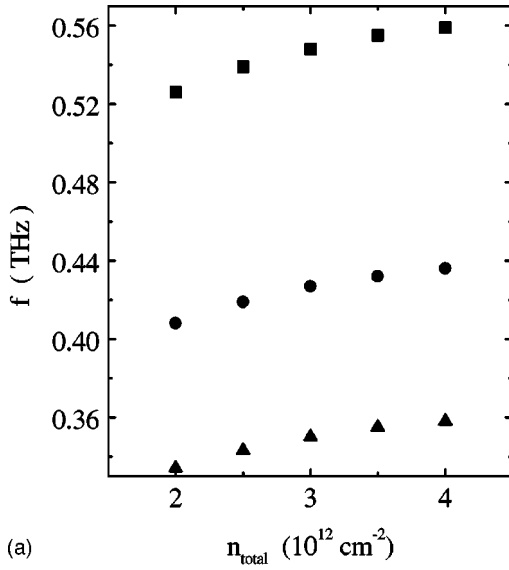


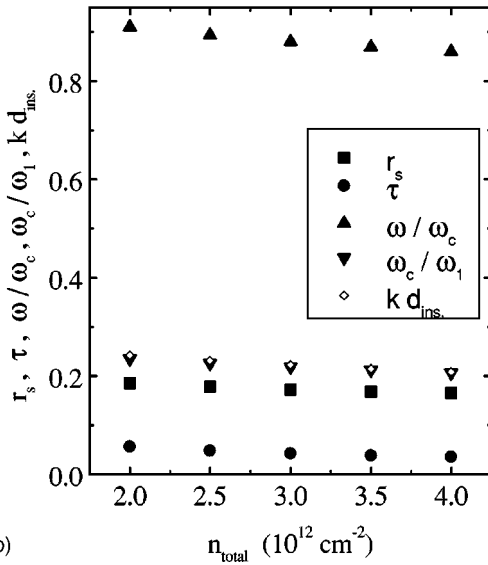
FIG. 4. For the parameter setting of Fig. 3 and for a reference mobility corresponding to the lowest curve in Fig. 3 ($50\,000 \text{ cm}^2/\text{V s}$) (*actual* mobility depends on total carrier density $\propto 1/\sqrt{n_{\text{total}}}$) the following parameters are plotted: $r_s \equiv k_{TF}/2k_F$, $\tau \equiv T/T_F$, the ratios of the frequencies of the low-frequency plasmon divided by the collision frequency (ω/ν_c), the collision frequency divided by the frequency of the idler plasmon (ν_c/ω_1), and the thickness of the insulator between the Q2DEG and the grating in terms of the wave number of the low-frequency plasmon (kd_{ins}): (a) for $T=77 \text{ K}$; (b) for $T=300 \text{ K}$.

frequency plasmons. However, because power transfer from the three-dimensional medium to the Q2DEG occurs through resonance, a sharp peak in the spectrum of the particular SRS process used for this purpose would be an advantage.

Another open question is the control over the three-dimensional plasma frequency. Because the three-dimensional plasma frequency depends on the effective mass and infrared refractive index, which in turn depend on the abundance of optically excited carriers (of effective mass ~ 1) and on the total carrier density, hence on the laser power, it is a rather complicated task to theoretically predict



(a)



(b)

FIG. 5. InSb as both the Q2DEG and the 3D medium for the same parameter setting as Fig. 3 except for the 3D refractive index $n_{r,3D}=4.0$, and the vacuum laser wavelength $\lambda_{laser,vacuum}=8 \mu\text{m}$: (a) dependence of the (linear) terahertz frequency on total carrier density for three values of the reference mobility [$\mu(n_{total}=10^{12} \text{ cm}^{-2})=80\,000, 100\,000, \text{ and } 120\,000 \text{ cm}^2/\text{V s}$ from top to bottom]; (b) parameters $r_s, \tau \equiv T/T_F, \omega/\omega_c, \omega_c/\omega_1, kd_{ins}$ versus the total carrier density for a reference mobility $\mu(n_{total}=10^{11} \text{ cm}^{-2})=100\,000 \text{ cm}^2/\text{V s}$. These results are valid for $T=77 \text{ K}$ but not extendable to 300 K because of the low-energy gap, given the present relatively short vacuum laser wavelength of $8 \mu\text{m}$.

conditions under which the three-dimensional plasma frequency will equal the quasi-two-dimensional pump frequency of a given wave number. The problem is aggravated by uncertainties about the lifetime of carriers optically excited into the conduction band of low-gap semiconductors, particularly in relation to the plasma period. Without any enhancement of the product of effective mass and permittivity the carrier density required for the conditions pertaining to Fig. 3(c) is in the $10^{16}\text{--}10^{17}$ range; see Fig. 3(d).

The essence of the present finding of three-plasmon inter-

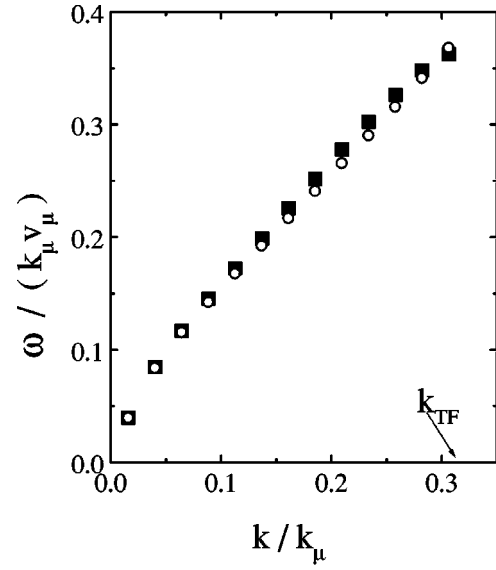


FIG. 6. Comparison between the lowest-order analytical approximation for the high-frequency plasmon dispersion equation [Eqs. (A8)] and the integral equation [Eq. (12)], for $r_s=0.16$ and $\tau \equiv T/T_F=0.16$. All other data have been obtained by computing the real root ω_r to the real part of the permittivity ϵ given by the full integral equation [Eq. (12)], and approximating the imaginary part of the frequency by $\gamma \approx -\text{Im}(\epsilon)/[\partial_{\omega_r} \text{Re}(\epsilon)]$.

action depends on the shift in real frequency caused by the linear momentum relaxation rate ν_c incorporated through a BGK model. This shift is due to the existence of a velocity drag and the absence of a corresponding dissipative process in the equation of continuity. Such a shift is possible, but of a different physical origin (ionization recombination) and hence would always be an independent physical quantity. The above-mentioned shift results in a drastic phase velocity reduction of the low-frequency plasmon enabling a resonance for low wave number ($k \ll k_s$) and with pump and idler wave numbers down to a finite fraction of the effective screening wave number of the low-frequency plasmon, which is the screening wave number calculated with the average of the semiconductor and insulator dielectric constants. Because the phase velocity of the excited low-frequency plasmon is approximately equal to the group velocity of the high-frequency plasmons, retardation effects are negligible, provided this group velocity, typically between one and several times the Fermi velocity, is small compared with the velocity of light, which is assumed here and which is true for the quantified examples. Frequency difference generation is predicted to result in a saturated amplitude of the low-frequency plasmon after approximately 1 or 2 ps and at a power level quantified by Fig. 8, which information might be used for an experimental test.

ACKNOWLEDGMENT

It is a pleasure to acknowledge Dr. Bun Lee for stimulating discussions and logistical support.

APPENDIX

We discuss the conditions under which the integral representation [Eq. (12)] of the high-frequency plasmon disper-

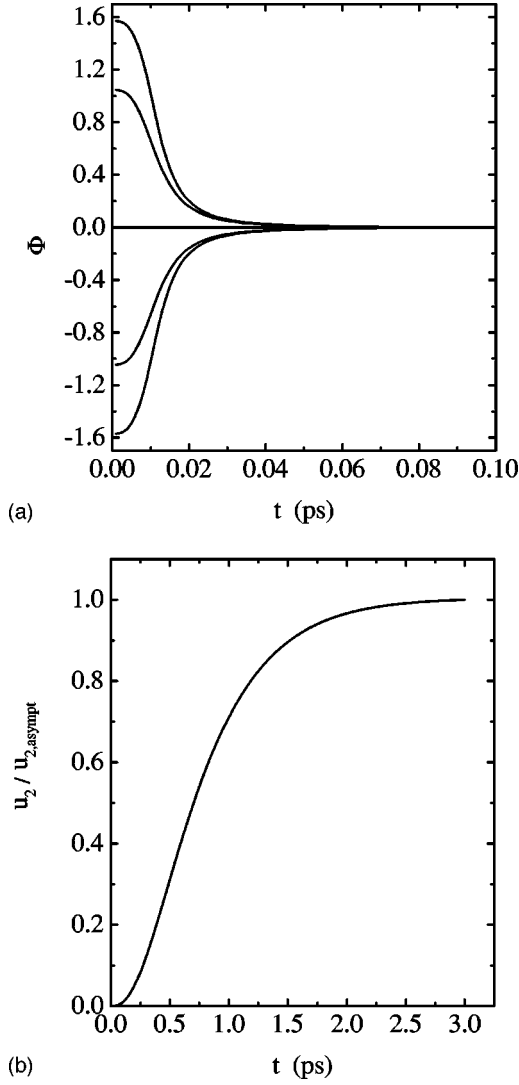


FIG. 7. Nonlinear evolution: (a) Time dependence of the phase $\hat{\Phi}$, essentially the phase difference between the normal modes, in Eqs. (44)–(47) for various initial conditions, demonstrating subpicosecond relaxation to zero. Parameters: $v_{01} = 0.579 \times 10^{12} \text{ s}^{-1}$, $v_{02} = v_{12} = 8.51 \times 10^{12} \text{ s}^{-1}$, $\omega_c = 5.09 \times 10^{12} \text{ s}^{-1}$, $u_{0m} = 0.03$, $\nu_d = 2.5 \times 10^{12} \text{ s}^{-1}$. The low-frequency plasmon amplitude saturates to the same value at a much later time (1–2 ps); (b) evolution of the normal mode of the low-frequency plasmon for the same case as in (a).

sion equation may be approximated through an expansion for low electron temperature. The kernel in the integral representation depends on the integration variable through $v_{\mu'}$ $\equiv (2\mu'/m)^{1/2}$. The relevant nontrivial integrals to be performed are

$$I_{\pm} \equiv \frac{k_{TF}}{k} \frac{1}{4\omega_q} (\omega_{\pm}^2 - k^2 v_{\mu}^2)^{1/2} J_{\pm}, \quad (\text{A1})$$

with the definition

$$J_{\pm} \equiv \int_{(-\beta\mu/2)}^{\infty} \frac{(1 - \alpha_{\pm}x)^{1/2}}{\cosh^2 x} dx, \quad (\text{A2})$$

where we defined $\alpha_{\pm} \equiv (2T/T_F)/(\bar{v}_{\phi, \pm}^2 - 1)$, an inverse measure of the closeness of the (Doppler-shifted) phase veloci-

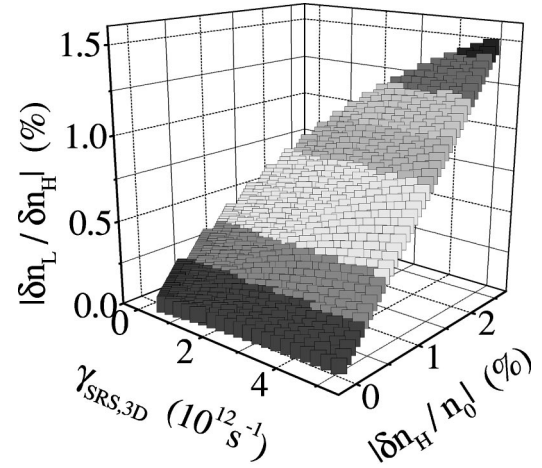


FIG. 8. Time-asymptotic ratio of the density fluctuations of the terahertz plasmon and the high-frequency plasmons in percent, as a function of both the density fluctuation relative to background density of the high-frequency plasmon (in percent) and the characteristic rate $\gamma_{SRS,3D}$ of the three-dimensional SRS (in units 10^{12} s^{-1}). Parameters as in Fig. 3 with the actual mobility equal to $10047 \text{ cm}^2/\text{Vs}$, and a density of $3 \times 10^{12} \text{ cm}^{-2}$. Other (dependent) parameters are $v_{01} = 5.79 \times 10^{12} \text{ s}^{-1}$; $v_{02} = v_{12} = 10^{12} \text{ s}^{-1}$; $\nu_c = 2.87 \times 10^{12} \text{ s}^{-1}$.

ties and the Fermi velocity in units of the thermal velocity. The real ($J_{\pm,r}$) and imaginary ($J_{\pm,i}$) parts are equal to

$$J_{\pm,r} = \frac{1}{\alpha_{\pm}} \int_{(-\alpha_{\pm}\beta\mu/2)}^1 \frac{(1-x)^{1/2}}{\cosh^2(x/\alpha_{\pm})} dx, \quad (\text{A3})$$

and

$$J_{\pm,i} = \alpha_{\pm}^{-1} \int_1^{\infty} \frac{(x-1)^{1/2} dx}{\cosh^2(x/\alpha_{\pm})}. \quad (\text{A4})$$

Provided $\alpha_{\pm} \ll 1$, $\cosh^{-2}(x/\alpha_{\pm}) \approx 0$ unless $x \ll 1$. Only then is the imaginary part exponentially small. For the full integral equation no *a priori* assumption is necessary, since Landau damping manifests itself through the disappearance of a real root to the real part of the permittivity, while if the solution can be obtained $\gamma \approx -\text{Im}(\epsilon)/\partial_{\omega}\text{Re}(\epsilon)$. In the expression for the real part of J_{\pm} the square root in the numerator can then be expanded for small $x \ll 1$. Keeping only the first three terms and partially integrating the second and third term we find

$$\begin{aligned} J_r = & \frac{1}{2} \tanh \frac{1}{\alpha_{\pm}} + \frac{1}{2} \left(2 + \frac{1}{\alpha_{\pm}^2 - 1} \right) \tanh \frac{T_F}{T} \\ & + \alpha_{\pm} \left(\ln \cosh \frac{1}{\alpha_{\pm}} - \ln \cosh \frac{T_F}{2T} \right) \\ & + \frac{1}{4} \alpha_{\pm}^2 \left[\int_0^{\infty} d\xi \frac{\xi^2}{\cosh^2(x)} \right. \\ & - (\alpha_{\pm}^{-2} + \alpha_{\pm}^{-1} + 1/2) e^{-2/\alpha_{\pm}} \\ & \left. - \left(\frac{1}{4} T_F^2/T^2 + \frac{1}{2} T_F/T + \frac{1}{2} \right) e^{T_F/T} \right]. \quad (\text{A5}) \end{aligned}$$

Here, the only remaining integral is equal to 0.8225. The degree of smallness of the imaginary part follows from the substitution $\cosh(\xi) \approx e^{|\xi|}/2$ under the same restriction:

$$J_i = \sqrt{2\pi} \alpha_{\pm} \exp(-2/\alpha_{\pm}), \quad (\text{A6})$$

which is exponentially small when $\alpha_{\pm} \ll 1$, i.e., when the difference between the phase velocity Doppler-shifted by $\pm \omega_q/2$ and the Fermi velocity is small compared with the thermal velocity. In conclusion, for $\alpha_{\pm} \ll 1$ and to within an error of order $\alpha_{\pm}^2/4$ the integrals J_{\pm} may be approximated by the above expressions. The high-frequency plasmon dispersion equation reduces to its zero-temperature limit when in addition $T/T_F \ll 1$, since then $J_{\pm} = 2$. The relative errors in the integrals J_{\pm} each are therefore half of the absolute values given above. The condition $\alpha_{\pm} \ll 1$ reflects the importance of finite temperature effects upon waves with a phase velocity that differs from the Fermi velocity by about the thermal velocity or less. With this approximation the permittivity becomes

$$\epsilon = 1 + \frac{k_{TF}}{k} \left(1 + \frac{\sqrt{\tilde{v}_-^2 - 1} - \sqrt{\tilde{v}_+^2 - 1}}{k/k_F} \right), \quad (\text{A7})$$

$$\omega = \sqrt{(1 + \delta)} \omega_{sc}, \quad (\text{A8})$$

where

$$\omega_{sc} \equiv \frac{(k_{TF}k + k^2)v_{\mu}}{(2k_{TF}k + k^2)^{1/2}} \quad (\text{A9})$$

is the semi-classical limit ($k/k_F \downarrow 0$) of the eigenfrequency and where

$$\delta \equiv \left(\frac{k^2}{2k_{TF}k_F} \right)^2 (1 + 2k_{TF}/k). \quad (\text{A10})$$

Because the errors are additive the combined relative error in the numerator involving the square roots in the above expression for the permittivity equals $\alpha^2/4$, where α by definition is the maximum of the α_{\pm} .

The above-derived simplified dispersion relation exhibits the well-known²³ first-order Taylor expansion in k/k_{TF} , i.e.,

$$\omega(k \ll k_{TF}) \approx \omega_{sc} \approx \left(1 + \frac{3}{4} \frac{k}{k_{TF}} \right) \sqrt{2kk_{TF}v_{\mu}}. \quad (\text{A11})$$

Even in the low-temperature regime it is only possible to satisfy both the real and imaginary parts of the dispersion equation for purely oscillatory waves when both Doppler-shifted phase velocities exceed the Fermi velocity in magnitude and provided the expression obtained by squaring both sides of the dispersion equation $\epsilon = 0$ as given by Eq. (A7) allows for non-negative values of the product of the two square roots occurring in it. The latter condition is, in terms of $\tilde{v}_{\phi} \equiv \omega/(kv_{\mu})$:

$$\tilde{v}_{\phi}^2 \geq 1 + \frac{1}{2} \left(\frac{k^2}{k_{TF}k_F} \right)^2 \left(1 + \frac{k_{TF}}{k} \right)^2 - \frac{1}{4} \left(\frac{k}{k_F} \right)^2. \quad (\text{A12})$$

In terms of wave number the above condition is met if and only if

$$k^3 + 2k_{TF}k^2 \leq 2k_{TF}^2k_F. \quad (\text{A13})$$

A quantitative comparison between the solutions of the integral form of the dispersion equation and even the lowest-order approximation in T/T_F given above shows agreement (see Fig. 6) within a few percent for the frequency and even better agreement for the (more relevant) group velocity up to the wave number at which the integral equation fails to have a solution altogether due to Landau damping. All results other than Fig. 6 given here are obtained from the full integral dispersion equation.

*Email: jpmondt@yahoo.com. Corresponding author: 2323B 38 Street, Los Alamos, NM 87544.

†Email: kimht45@hotmail.com

‡Email: kykang@etri.re.kr

¹K. Kempa, P. Bakshi, J. Cen, and H. Xie, Phys. Rev. B **43**, 9273 (1991).

²P. Bakshi and K. Kempa, Superlattices Microstruct. **17**, 363 (1995).

³B. Y.-K. Hu and J.W. Wilkins, Phys. Rev. B **43**, 14 009 (1991).

⁴M. Dyakonov and M. Shur, Phys. Rev. Lett. **71**, 2465 (1993).

⁵M. Dyakonov and M. Shur, IEEE Trans. Electron Devices **43**, 1640 (1996).

⁶L. Fedichkin, V. Ryzhii, and M. Willander, in *Proceedings of the 2nd International Workshop on the Physics and Modeling of Devices Based on Low-Dimensional Structures*, 12–13 March 1998, Aizu-Wakamatsu, Japan (IEEE Comput. Soc., Los Alamitos, CA, 1998).

⁷D.C. Montgomery and D.A. Tidman, *Plasma Kinetic Theory* (McGraw-Hill, New York, 1964).

⁸K.I. Golden and De-Xin Lu, Phys. Rev. A **45**, 1084 (1992); erratum in Phys. Rev. E **47**, 4632 (1993).

⁹K. Hirakawa, I. Wilke, K. Yamanaka, H.G. Roskos, M. Vosseburger, F. Wolter, C. Waschke, H. Kurz, M. Grayson, and D.C.

Tsui, Surf. Sci. **361/362**, 368 (1996).

¹⁰J.A. Armstrong, N. Bloembergen, J. Ducuing, and P.S. Pershan, Phys. Rev. **15**, 1918 (1962).

¹¹H. Wilhelmsson, L. Stenflo, and F. Engelmann, J. Math. Phys. **11**, 1738 (1970).

¹²J. Weiland and H. Wilhelmsson, *Coherent Non-Linear Interaction of Waves in Plasmas* (Pergamon Press, Oxford, 1977), Chap. 6.

¹³M. Sheik-bahaei, M.P. Hasselbeck, and H.S. Kwok, J. Opt. Soc. Am. B **3**, 1082 (1986).

¹⁴S. Dubey and S. Ghosh, J. Phys. I **7**, 1445 (1997).

¹⁵B. Kh. Bairamov, V.D. Timofeev, V.V. Toporov, and Sh.B. Ubaidullaev, Fiz. Tverd. Tela (Leningrad) **20**, 3321 (1978) [Sov. Phys. Solid State **20**, 1916 (1978)].

¹⁶D. von der Linde, M. Maier, and W. Kaiser, Phys. Rev. **178**, 11 (1969).

¹⁷A.C. Calder and A.J. Barnard, Phys. Fluids **31**, 2335 (1988).

¹⁸M.P. Mikhailova, in *Handbook Series on Semiconductor Parameters*, edited by M. Levinshteyn, S. Romyantsev, and M. Shur (World Scientific, Singapore, 1996), Vol. 1, Chap. 7.

¹⁹A.L. Fetter, Ann. Phys. (N.Y.) **81**, 367 (1973).

²⁰E.M. Lifschitz and L.P. Pitaevskii, Vol. 10 *Physical Kinetics of Landau and Lifschitz: Course of Theoretical Physics* (Pergamon Press, Oxford, 1981).

- ²¹P.F. Maldague, *Surf. Sci.* **73**, 296 (1978).
- ²²D.A. Dahl and L.J. Sham, *Phys. Rev. B* **16**, 651 (1977).
- ²³T. Ando, A.B. Fowler, and F. Stern, *Rev. Mod. Phys.* **54**, 437 (1982).
- ²⁴J.M. Burgers, in *Flow Equations for Composite Gases*, Vol. 11 of Applied Mathematics and Mechanics Series (Academic Press, New York, 1969), Chap. 6, Sec. 47.
- ²⁵P.L. Bhatnagar, E.P. Gross, and M. Krook, *Phys. Rev.* **94**, 511 (1954).
- ²⁶A.L. Fetter, *Ann. Phys. (N.Y.)* **82**, 1 (1974).
- ²⁷T. Jungwirth and A.H. MacDonald, *Phys. Rev. B* **53**, 7403 (1996).
- ²⁸Lian Zheng and S. Das Sarma, *Phys. Rev. B* **53**, 9964 (1996).
- ²⁹R.N. Gurzhi, A.N. Kalinenko, and A.I. Kopeliovich, *Phys. Rev. B* **52**, 4744 (1995).
- ³⁰T. Ando, *J. Phys. Soc. Jpn.* **54**, 2676 (1985).
- ³¹F.J. Ohkawa and Y. Uemura, *J. Phys. Soc. Jpn.* **37**, 1325 (1974).
- ³²Y. Takada, K. Arai, N. Uchimura, and Y. Uemura, *J. Phys. Soc. Jpn.* **49**, 1851 (1980).
- ³³Yu. Goldberg, in *Handbook Series on Semiconductor Parameters*, edited by M. Levinshteyn, S. Rumyantsev, and M. Shur (World Scientific, Singapore, 1996), Vol. 1, Chap. 9.
- ³⁴C.S. Liu and V.K. Tripathi, *Interaction of Electromagnetic Waves With Electron Beams and Plasmas* (World Scientific, Singapore, 1994), Chap. 7.